Reducing Spring back in Sheet Metal Forming Using Compression and Shear

Jacob Wettstein
University of Michigan, Department of Mechanical Engineering

1. Introduction

Incremental sheet forming is a sheet metal forming technique in which sheet metal is formed into a final workpiece through a series of small deformations in the part[1]. It consists of a round-tipped deforming tool that progressively shapes a metal sheet into a final part through a series of small deformations. In some cases, a supporting tool is used to aid the deforming tool in making these deformations. Figure 1 shows a simple diagram of this process. Though it does take longer than a standard sheet forming process, it is beneficial because it requires no dedicated tooling, reducing the cost per part. Therefore, it can be a good solution for low volume sheet metal part production. However, the presence of springback, which is the tendency of sheet metal parts to want to return to their original shapes after being deformed[2], leads to geometric inaccuracies in the final part dimensions[3]. These inaccuracies are more problematic with Incremental Sheet Forming as opposed to standard sheet metal forming because Incremental Sheet Forming involves a series of deformations that each introduce geometric inaccuracy into the part.

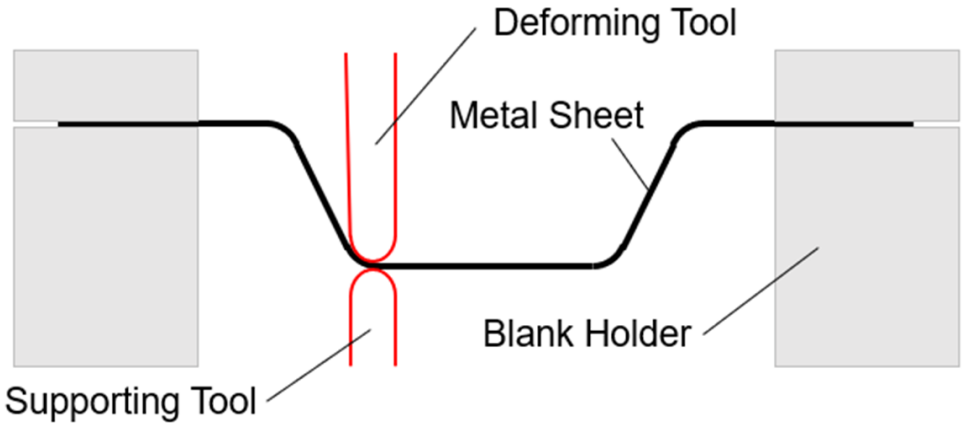

Fig. 1. Diagram of incremental sheet forming process.

2. Objectives

In this project, the first goal was to construct theoretical models of two bending scenarios, namely simple bending and simple compression. These scenarios will be outlined in more detail in the Methodology section. After developing these models, the next focus was to validate them by constructing a test rig and experimentally introducing and measuring spring back in each of the two scenarios. Given these analytical and experimental results, we could then assess the accuracy of rapid-to-calculate analytical spring back models derived from mathematical theory of plasticity. Another goal was to conduct additional experiments to investigate the effect of shear stress in reducing spring back in sheet metal forming. The final objective was to conduct finite element simulations of the same procedures performed in the experimental testing to determine how accurate numerical approaches can be in predicting spring back.

3. Methodology

There were three approaches taken to model spring back in sheet metal forming. Section 3.1 describes how theoretical models of sheet metal bending were derived. Section 3.2 describes the physical experiments performed to quantify springback in strips of 1100 Aluminum, including equipment design and sample preparation. Section 3.3 discusses the FEA simulations that the physical experiments could be compared against.

3.1. Analytical Predictions

Before conducting experiments or performing finite element simulations, a theoretical framework was developed using analytical approaches. The following subsections describe the concepts used to predict the springback levels for each of the cases of interest, namely simple bending and simple compression.

3.1.1. Simple Bending

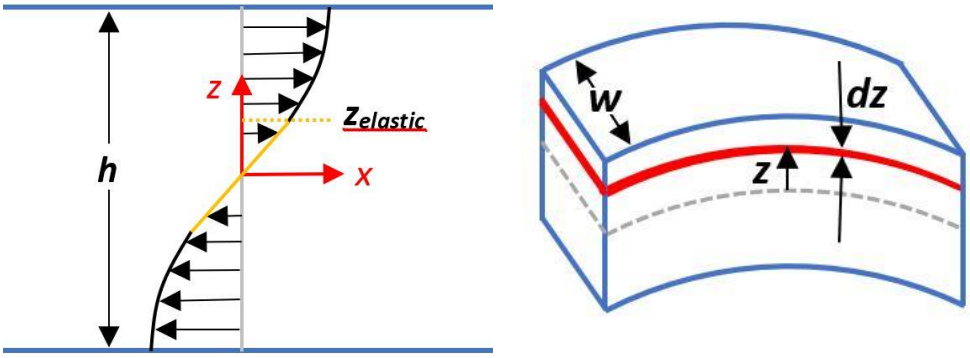

Fig. 2. Stress distribution through the thickness of the part (left) and labeled full-width element (right). The coordinate system indicated in the above diagrams will be used as the convention whenever a particular axis direction is referenced in this paper.

When a strip of aluminum is bent and thus, a moment is applied, a stress distribution develops across the thickness of the part, as shown in Figure 2. Each incremental element of this cross-section is associated with an internal force $dF_x = \sigma_x w\, dz$ with the $w\, dz$ part of that expression representing the area on which the stress, σ_x, acts. Multiplying the internal force associated with an element by the lever arm z for the element results in that element's contribution to the overall applied bending moment. This contribution can be expressed as $dM = z\, dF_x = z\, \sigma_x w\, dz$. The overall bending moment is thus given by Equation 1[2].

$$M_{applied} = \int_{-h/2}^{h/2} (z\sigma_x w) dz \quad [1]$$

Because the part contains both an elastic region and plastic region, the expression for σ_x differs between the two regions. Equation 2 provides the expression for σ_x in the elastic region. To develop an expression for σ_x in the plastic region, tensile testing was conducted on Aluminum 1100, the same material that will be used for experimental testing, and least squares fitting was employed to determine the most accurate strain hardening approximation, which proved to be the Ludwik model. The tensile testing will be

discussed in more detail in Section 3.3.1. To simplify the calculations, the plane strain assumption was used. This approximation states that the strain of the material in one direction, the *y* direction in the case of Figure 1, is zero, which could be made because the widths *w* of the strips being analyzed were significantly greater than their thicknesses *h*. Given this assumption, the Ludwik approximation could be written as Equation 3.

$$\sigma_{x,\,elastic} = E'\varepsilon \quad [2]$$

$$\sigma_{x,\,plastic} = \frac{2}{\sqrt{3}}(Y + n\varepsilon^{m}) \quad [3]$$

In the above two equations, *E'* denotes the plane strain Young's Modulus, ε is the strain, *Y* is the yield strength, and *n* and *m* are parameters of the Ludwik strain hardening fit. The $\frac{2}{\sqrt{3}}$ in Equation 3 arose from the plane strain assumption. Equation 4 gives an expression for the strain ε.

$$\varepsilon = \frac{z}{r} \quad [4]$$

where *r* is the radius of curvature of the bent part. Equation 1 could be written as the summation of two integrals, one for the elastic region and one for the plastic region, as shown below in Equation 5. Equation 4 was also substituted in for the strains.

$$M_{applied} = \frac{2wE'}{r}\int_{0}^{z_{elastic}} z^2 dz + \frac{4}{\sqrt{3}}w\int_{z_{elastic}}^{h/2} z(Y + n(\frac{z}{r})^{m})dz \quad [5]$$

An expression for the cutoff point, $z_{elastic}$, between the elastic and plastic regions could be determined by noting that when $z = z_{elastic}$, $\sigma_x = Y$. Combining this statement with Equations 2 and 4 led to the following expression for $z_{elastic}$.

$$z_{elastic} = \frac{Yr}{E'} \quad [6]$$

Solving Equation 5 and simplifying resulted in Equation 7 below for the applied moment.

$$M_{applied} = \frac{2wY^3r^2}{3E'^2} + \frac{2}{\sqrt{3}}wY(\frac{h^2}{4} - (\frac{Yr}{E'})^2) + \frac{4wn}{(\sqrt{3})r^m(m+2)}((\frac{h}{2})^{m+2} - (\frac{Yr}{E'})^{m+2}) \quad [7]$$

The plane strain Young's Modulus is given by the following equation.

$$E' = \frac{E}{1-\nu^2} \quad [8]$$

where *E* is the material's Young's Modulus and *ν* is the material's Poisson's ratio. The elastic stresses in the part generate a springback moment that acts in the opposite direction as the applied moment. When the part is released, it unloads elastically, so the change of stress is given by the equation below.

$$\Delta\sigma_x = E'\Delta\varepsilon = E'(\frac{z}{r} - \frac{z}{r'}) \quad [9]$$

In Equation 9, *r'* represents the radius of the part after springback. Using the same relationship in Equation 1, the springback moment, or change of bending moment, could be written as the following equation.

$$\Delta M = 2wE' \int_0^{h/2} z^2 \left(\frac{1}{r} - \frac{1}{r'}\right) dz = \left(\frac{wE'h^3}{12}\right)\left(\frac{1}{r} - \frac{1}{r'}\right) \quad [10]$$

After springback, an equilibrium has been established with the total bending moment equal to zero. Thus, $M_{applied} - \Delta M = 0$. By setting the applied moment equation equal to the springback moment equation, the following relationship between loaded radius and unloaded radius could be established.

$$r' = \frac{h^3 r E'^3 (m+2)}{h^3 E'^3 (m+2) + (-8r^2 Y^3 - 2(\sqrt{3}) Y (h^2 E'^2 - 4r^2 Y^2)) r(m+2) - 16\sqrt{3} n \left(\left(\frac{h}{2}\right)^{m+2} - \left(\frac{Yr}{E'}\right)^{m+2}\right) E'^2 r^{-m+1}} \quad [11]$$

With the above relationship, the radius of curvature of a sheet of metal after springback could be predicted based on its radius of curvature before springback, after it has been loaded.

3.1.2. Simple Compression

In simple bending, there was no stress in the *z* direction. The only stress in simple bending arose when the metal strip was bent, which created stresses in the *x* direction. In the simple compression scenario, however, there was a compressive stress σ_z in the loading phase. This compression stress contributed to the bending stress in the *x* direction, altering Equation 3 to the following equation.

$$\sigma_{x,\,plastic} = \frac{2}{\sqrt{3}} \left(Y + n\varepsilon^m\right) + \sigma_z \quad [12]$$

This equation resulted in the following equation for the applied moment.

$$M_{applied} = \frac{2wY^3 r^2}{3E'^2} + \frac{1}{2} w \left(\frac{2}{\sqrt{3}} Y + \sigma_z\right)\left(\frac{h^2}{4} - \left(\frac{Yr}{E'}\right)^2\right) + \frac{2wn}{\sqrt{3} r^m (m+2)} \left(\left(\frac{h}{2}\right)^{m+2} - \left(\frac{Yr}{E'}\right)^{m+2}\right) \quad [13]$$

By again equating the spring back moment to the applied moment, an expression for the unloaded radius of curvature in terms of the radius of curvature could be derived, as shown below.

$$r' = \frac{2h^3 r E'^3 (m+2)}{2h^3 E'^3 (m+2) - 16r^3 Y^3 (m+2) - \sqrt{3}(2Y + \sigma_z\sqrt{3})(h^2 E'^2 - 4Y^2 r^2) r(m+2) - 16\sqrt{3} n \left(\left(\frac{h}{2}\right)^{m+2} - \left(\frac{Yr}{E'}\right)^{m+2}\right) E'^2 r^{-m+1}} \quad [14]$$

3.2. Physical Experiments

A test rig was constructed that would apply bends to strips of 1100 Aluminum and allow for the strips' radii of curvature to be measured. These measurements were used to quantify the levels of springback for strips of aluminum under various conditions. Three primary testing conditions were performed with the rig. The first two conditions directly corresponded to the analytical models developed and discussed in the previous section, namely simple bending and simple compression. A third case was also tested experimentally. In this condition, shear stress was introduced to the aluminum strips during bending. Each of these testing conditions will be discussed in more detail within the following subsections.

3.2.1. Equipment Design

Strips of aluminum were fed between two pairs of rollers. Each roller within a pair could be rotated about the same axis and a rotation of one pair of rollers resulted in the same magnitude of rotation in the other pair of rollers because they were connected through a set of gears. When one of these roller sets was rotated, and thus the other pair in the opposite direction, a bend would be imparted in the strip of aluminum. The degree of bending depended on the amount of rotation performed by the rollers. The entire rig assembly is visible in Figure 3.

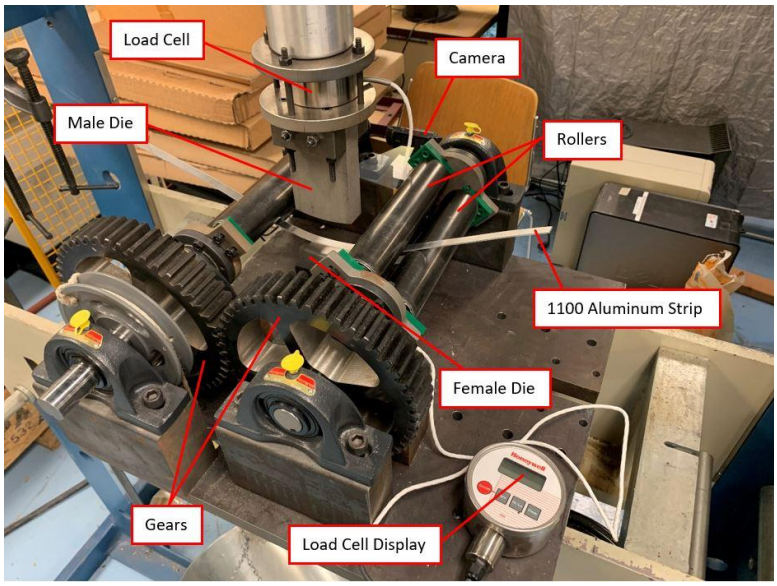

Fig. 3. Diagram of experimental test rig

For simple compression tests, a female die was mounted to the base plate of the rig and a matching male die was bolted into a support structure directly above the female die. Each die consisted of a 304 stainless steel bar with a certain radius arc machined into one end of the bar. Three pairs of compression dies were created: one with a five-inch arc, one with a six-inch arc, and one with a seven-inch arc. Figure 4 shows one of these die pairs.

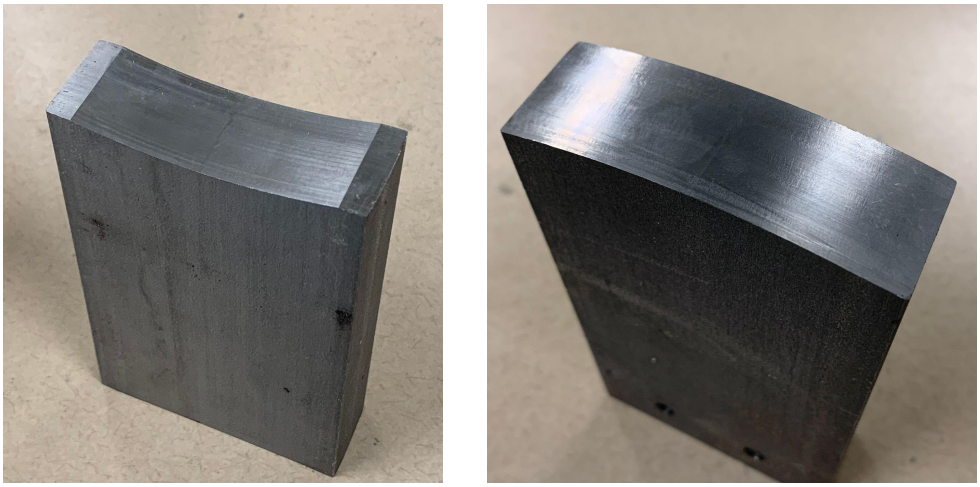

Fig. 4. Lower female standard compression die (left) and upper male standard compression die (right).

The male die could be moved up and down via a 60-turn hydraulic press to apply compressive force to the strips of aluminum. To measure these compressive forces, a load cell was contained in a steel housing directly above the male die. For each test, the aluminum strip was inserted between the rollers, the rollers were rotated to bend the aluminum strips until they made contact with the female, or lower, die, and the upper male die was lowered until it applied a certain compressive force to the aluminum strip. As the male die applied force to the aluminum strips, the load cell was compressed, allowing it to record the maximum force of compression that it experienced in that test. After compression, the upper die was raised to its original height and the rollers were manually rotated backwards enough for the strips of aluminum to spring back. Figure 5 shows the initial state of the rollers and aluminum strip after the strip has just been inserted between the rollers while Figure 6 demonstrates how the compression experiments were conducted.

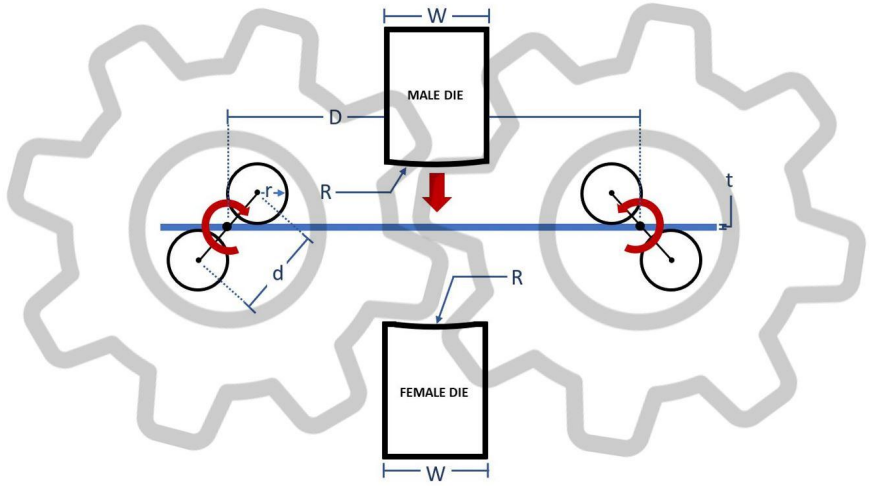

Symbol	Value
D	202 mm
d	54 mm
R	152.4 mm
r	24.20 mm
W	76.2 mm
t	1.27 mm

Fig 5. Diagram of rollers with table showing the corresponding values in compression experiments.

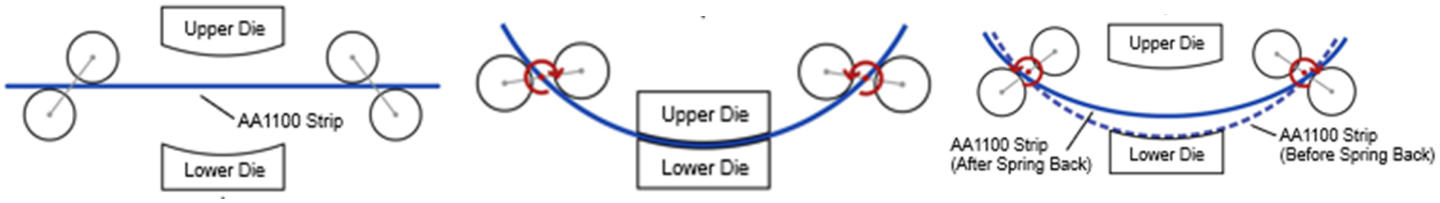

Fig 6. Diagram showing simple compression experimental procedure. Aluminum strip inserted between rollers (left), strip is bent as the rollers rotate and the upper die is lowered to apply compressive force (middle), and upper die is raised, allowing the strip to spring back.

Shear testing was conducted in a similar fashion to the simple compression testing. Shear stresses are created when a torque is applied to a part. To create this torque, a specialized pair of compression dies was machined with a 15° angle that would cause the aluminum strips to twist, and therefore become torqued, as they were compressed. One shear die pair with a six-inch arc was created for this phase of the testing, which is shown in Figure 7 along with the angle machined into the dies.

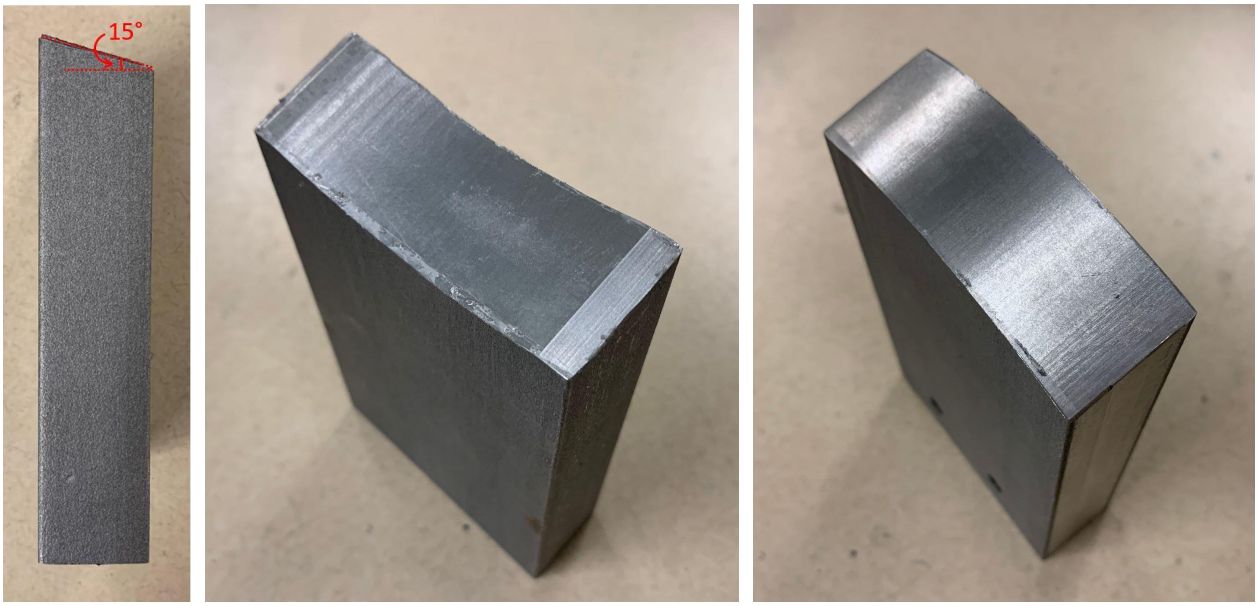

Fig. 7. Side view of lower female shear die with angle of die labeled (left), isometric view of lower female shear die (middle), and isometric view of upper male shear die (right).

To conduct each of these shear stress experiments, the aluminum strip was inserted between the rollers, the rollers were rotated to bend the aluminum strips until they contacted the female shear die, and the upper die was lowered until it applied a certain compressive force to the aluminum strip. The upper male die was then raised, and the strip of aluminum was unloaded to measure its spring back.

To perform simple bending tests that did not involve compression, the lower die was removed from the base plate and a pulley was attached to one set of rollers. When a specific weight was added to the bucket attached to this pulley, a corresponding moment would be created that would rotate the rollers by an amount dependent upon how much weight was in the bucket. For separate tests, various weights were used to create different bending moments, resulting in strips that were bent to various radii. To unload the strips, the weights were removed from the bucket and the rollers were rotated backwards to allow the strips to spring back.

3.2.2. Sample Preparation

Sheets of 1100 Aluminum were purchased for experimental testing and a power shear was used to cut the sheets into strips, each with a width of 12 mm. The sheets were cut such that the grains in the aluminum were always parallel to the long lengths of the strips.

3.2.3. Evaluating Springback

To quantify the level of spring back for each strip of sheet metal that underwent either a simple bending, simple compression, or shear test, a camera was mounted next to the test rig such that the curvature of the strips was visible. Measuring the radius of curvature of a strip required taking a picture of the strip with the camera, an example of which is shown in Figure 8.

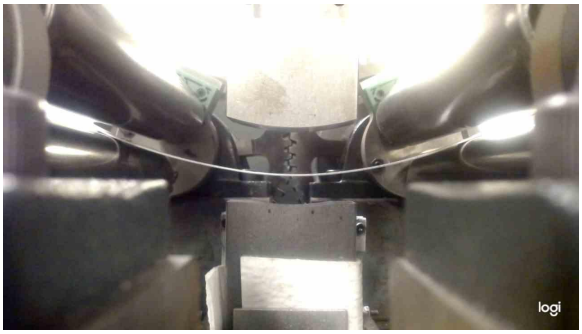

Fig. 8. State of aluminum strip after springback from the point of view of camera.

A MATLAB script was developed that takes a picture as input and allows the user to mark points on the curve to be measured in that picture. The script outputs the radius of curvature. Because the aluminum strips that underwent simple bending testing weren't compressed between dies of specific radii, for each test, the loaded radius of curvature needed to be measured in addition to the unloaded radius of curvature. To accomplish this, a picture was taken in the loaded state and an additional picture was taken in the unloaded state after the strip had experienced spring back. These pictures were then used to determine the unloaded and loaded radii of curvature, which were used to calculate the level of spring back in that particular test.

The loaded radius of curvature for each strip undergoing either simple compression testing or shear testing was the same as the radius of curvature of the arc machined into the particular die pair used for that test. Therefore, only the unloaded radius of curvature needed to be measured for simple compression and shear tests.

3.3. Simulations

Finite element simulations were conducted using Abaqus. For simple bending and simple compression tests, each aluminum strip was modeled as a 2D deformable body with the plane-strain assumption and meshed using about 400 plate elements. The plane-strain assumption was valid because the thickness of each strip was less than one sixth of the width of each strip. The strips modeled in shear tests needed to be created as 3D deformable bodies because the geometry of the shear dies could only be created in 3D. These strips were meshed using about 2,000 solid elements. Before Abaqus simulations were performed, tensile tests were conducted to define the plastic material properties of the 1100 Aluminum material that was to be used in the simulations. The coefficient of friction between the aluminum strips and the rollers also needed to be determined. The methodologies for determining these two properties are discussed in the following two subsections.

3.3.1. Tensile Testing

Three 1100 Aluminum specimens were cut from the same material that was used in experimental testing using a wire EDM and pulled on an Instron with an extension rate of 0.2 mm/s. The data from these tests was used to obtain the following flow curve in Figure 9.

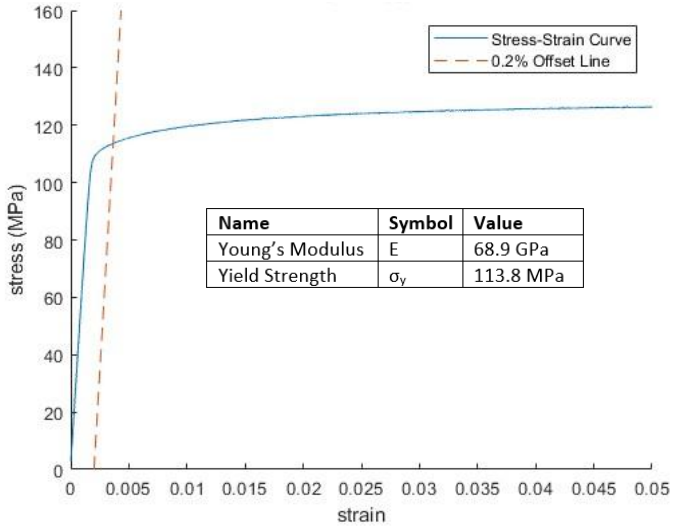

Fig. 9. Stress-strain curve used to define material properties of 1100 Aluminum in Abaqus simulations. The 0.2% offset line is also labeled. The stress at which the 0.2% offset line and stress-strain curve intersect gives the yield strength of the material, which is documented along with the known Young's Modulus of the material.

3.3.2. Coefficient of Friction Determination

As shown in Figure 3, the experimental setup consists of two pairs of rollers. A side view diagram of one such pair is shown below in Figure 10.

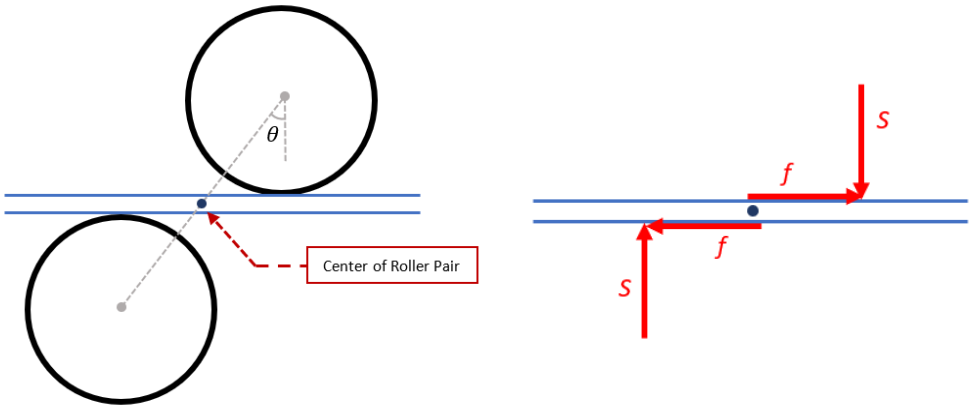

Fig. 10. Diagram of roller set with strip of aluminum in place between rollers (left) and forces acting on aluminum strip (right). *S* is the reaction force applied by the rollers to the strip and *f* is the friction force between the roller and strip.

In order to determine the coefficient of friction between the aluminum strip and roller, the moments around the center of the roller set were summed as the roller set was loaded. Before summing these moments, the moment arms of *S* and *f*, L_S and L_f, respectively, were determined. These two equations are shown below.

$$L_S = \frac{d}{2} sin(\theta) \quad [15]$$

$$L_f = \frac{h}{2} \quad [16]$$

where d is the distance between the center points of each roller in a set and h is the thickness of the sheet. The angle θ is labeled in Figure 7 and was found to be 0.603 radian. Summing the moments around the center of the roller set produced Equation 17 for the total moment $M_{loading}$.

$$M_{loading} = -2(S \cdot L_S + f \cdot L_f) = -Sdsin(\theta) - \mu Sh \quad [17]$$

In the above equation, the friction force f was replaced by the product of the coefficient of friction and the force S. In unloading, the only difference in the above equation is that the direction of the friction force is reversed, leading to the following equation for the unloading moment, $M_{unloading}$.

$$M_{unloading} = 2(-S \cdot L_S + f \cdot L_f) = -Sdsin(\theta) + \mu Sh \quad [18]$$

Since S is constant in both Equations 17 and 18, those two equations were combined using S to form Equation 5 below, which was rearranged to solve for μ.

$$\mu = \frac{dsin(\theta)(M_{loading} - M_{unloading})}{t(M_{loading} + M_{unloading})} \quad [19]$$

The coefficient of friction was used to define interactions between the strip of aluminum and each roller in simulation.

4. Results

The following subsections will detail the results that were obtained analytically and experimentally. Section 4.1 will draw comparisons between the theoretical model and experimental results. Section 4.2 will discuss the effect of shear stress in reducing springback. Section 4.3 will briefly discuss the FEA simulations that were conducted.

4.1. Theoretical Model Accuracy

After constructing theoretical models for both the simple bending and simple compression cases and obtaining experimental data for each, the data was plotted on top of the models. Figure 11 shows the results for simple bending.

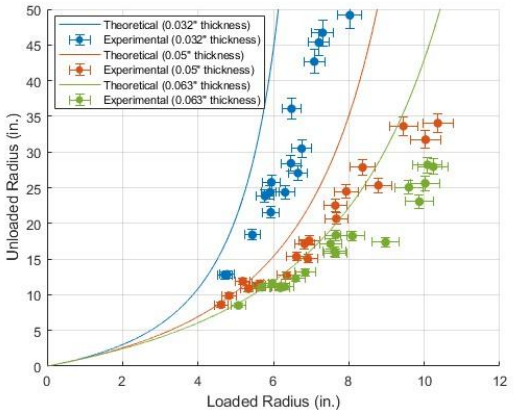

Fig. 11. Plot of experimental and analytical results for each of the three sheet metal thicknesses tested. The theoretical models tended to overestimate the experimental data.

While the general trend in the theoretical models matches those found in experimental data, there are some stark discrepancies between the two, namely that the theoretical models overestimated the experimental data for each of the three sheet metal thicknesses tested. While not ideal, because the primary objective was to show how analytical models could be used to predict spring back levels in sheet metal forming, the theoretical models were "calibrated" such that they would better match the experimental data. This was done by altering the yield used in these models. The yield strength that was found to produce more desirable theoretical models was 86 MPa, a decrease of about 30 MPa from the original yield strength of 113.8 MPa. The new flow curve with this yield strength is shown in Figure 12 while the updated comparison between analytical and experimental data is shown in Figure 13.

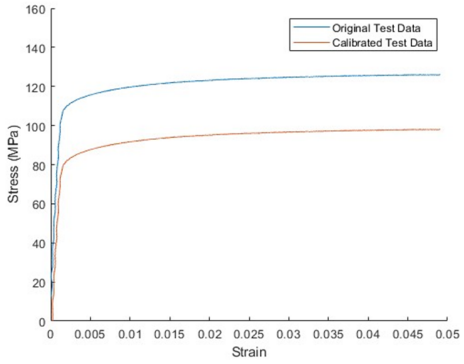

Fig. 12. Flow curve from tensile testing showing the original data and the "calibrated" data with 86 MPa as the "calibrated" yield strength.

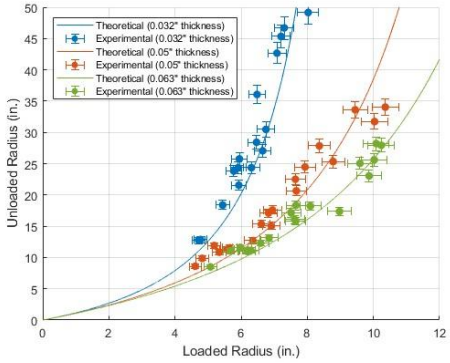

Fig. 13. Plot of experimental and analytical results with the theoretical models having been obtained using the "calibrated" yield strength.

Similarly, the theoretical model for simple compression was plotted on the same set of axes as the experimental data for simple compression. Again, before the calibration, the theoretical model overestimated the experimental data while after calibration, the analytical and experimental data more closely aligned. Calibration was performed the same way as in simple bending, by adjusting the yield strength to be 86 MPa. Figures 14 and 15 show the comparison before calibration and after calibration, respectively.

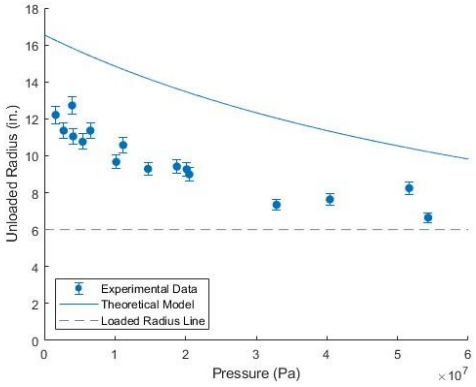

Fig. 14. Flow curve from tensile testing showing the original data and the "calibrated" data with 86 MPa as the "calibrated" yield strength.

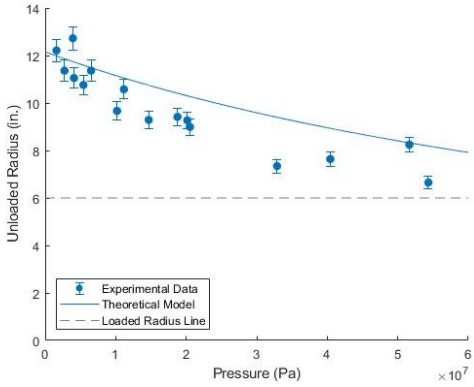

Fig. 15. Plot of experimental and analytical results with the theoretical models having been obtained using the "calibrated" yield strength.

4.2. Using Shear Stress to Reduce Spring Back

Experimental tests were also conducted using the specialized dies described in the Methodology section to impart shear stress into the strips of aluminum as they were bent. These data were plotted on the same set of axes as the simple compression tests and the results are shown below.

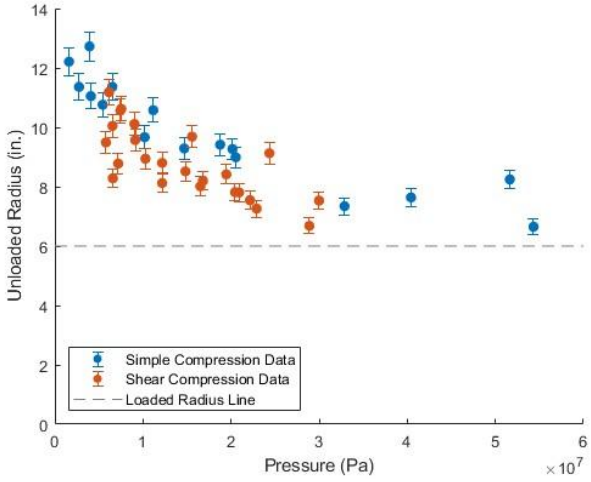

Fig. 16. Plot shear data and compression data.

As shown in Figure 11, there isn't a particularly noticeable reduction in spring back when the shear dies were used, so this data can't be used to conclude that shear stress, particularly shear stress in the *yz* direction, will mitigate spring back in sheet metal forming.

4.3. FEA Simulations

Unfortunately, there was insufficient time to extract meaningful data from the FEA simulations. However, these simulations did show that spring back in sheet metal forming can be modeled numerically. The implications of this will be discussed in the next section.

5. Conclusions

The results of this project demonstrated that with appropriate calibration, analytical methods, specifically plasticity theory, can be used to develop theoretical models that can accurately predict the level of spring back in sheet metal forming. This entails that analytical models can provide the means to implement a closed loop system in incremental sheet forming. This means that if a manufacturer would like to use incremental sheet forming to bend a sheet of metal to a specified radius, for example, analytical methods can inform the machine how much to bend the sheet such that after spring back, the resulting radius of curvature matches that specified by the operator. While numerical methods can also perform this function, the advantage of using analytical methods is that analytical methods are much quicker than numerical models and have the potential to be as accurate.

To further investigate spring back, additional FEA simulations will be conducted and its results will be compared to experimental data to determine how accurate numerical methods can be in predicting spring back in sheet metal forming. Having the ability to predict spring back both numerically and analytically will allow for additional analysis to be performed on the cost benefit of using numerical methods to model spring back during an incremental sheet forming process as opposed to analytical methods. Also, the effect of shear stress in reducing spring back will be investigated more thoroughly and theoretical models involving shear stress will be constructed to compare against experimental data. The work completed thus far in this project has laid the groundwork for these aspects of future investigation to be pursued.

6. References

[1] Boileau, J.; Kridli, G., *Materials, Design, and Manufacturing for Lightweight Vehicles*, 2021, 2, 316-318

[2] Li, M.; Wagoner, R.; Wang, J., "Springback," 2006

[3] Choubey, V.; Dwivedi, J.; Kumar, S.; Lal, R.; *Materials Today: Proceedings*, "Study of Factors Affecting Springback in Sheet Metal Forming and Deep Drawing Process, 2018, 5, 2